

Improving Optical Gyroscope Sensitivity Using a Fast Light Regime

A thesis submitted in partial fulfillment of the requirement
for the degree of Bachelor of Science in Physics from
The College of William and Mary

by

Owen R. Wolfe

Accepted for Honors
(Honors or no-Honors)

Eugeniy E. Mikhailov
Eugeniy E. Mikhailov, Physics

Henry Krakauer
Henry Krakauer, Physics

Gunter Luepke
Gunter Luepke, Applied Science

Williamsburg, VA
May 3, 2016

Improving Optical Gyroscope Sensitivity Using a Fast Light Regime

Owen Wolfe

Advisor: Eugeny E. Mikhailov

May 5, 2016

1 Abstract

Optical gyroscopes use Sagnac interferometry to make precise measurements of angular velocity. Increased gyroscope sensitivity will allow for more accurate control of aerospace systems and allow for more precise measurements of the Earth's rotation. Severalfold improvements to optical gyroscope sensitivity were predicted for fast light regimes ($n_g < 1$). We evaluated the feasibility of these improvements in the N-bar dual pump scheme in ^{87}Rb vapor. We were able to modify the stimulated gyroscope response via tuning the experimental parameters. Gyroscope sensitivity was shown to be dependent on several parameters including pump power, pump detuning, and vapor density.

Contents

1	Abstract	1
2	Introduction	3
2.1	Motivation	3
2.2	Background	3
2.2.1	The Sagnac effect	3
2.2.2	Laser Gyroscopes	4
2.2.3	Fast Light	5
3	Experiment	10
3.1	Optical Apparatus	10
3.2	Measuring Gyroscope Sensitivity	13
3.3	Control Systems	14
3.4	Pump Power Control	15
4	Results	15
4.1	Low Power Regime	15
4.1.1	Initial D1 Detuning Dependence	15
4.1.2	Initial D2 Detuning Dependence	17
4.1.3	D1 Detuning Dependence under improved D2 Detuning Conditions.	19
4.1.4	D2 Power Dependence	20
4.1.5	Vapor Density Dependence	22
4.1.6	Finesse Dependence	24
4.1.7	Low Power Conclusions	25
4.2	High Power Regime	25
4.2.1	D2 detuning Dependence (High Power Regime)	25
4.2.2	Pump Power Dependence	27
4.2.3	High Power Conclusions	28
5	Discussion	29
6	Conclusions	30
7	Acknowledgments	31

2 Introduction

2.1 Motivation

Historically, gyroscopes have been large top like devices that rely on the conservation of angular momentum to maintain original spatial orientation. In the 1970s, optical gyroscopes became popular for certain navigational applications [1]. Optical gyroscopes rotate freely with the device and provide measurements of angular velocity rather than providing a fixed reference for spatial orientation.

In aviation systems gyroscopes are used to stabilize aircraft trajectories. In environments where external position references such as GPS are unavailable, gyroscopes can be used in concert with other sensors such as accelerometers to employ a navigational method called inertial navigation [2]. Inertial navigation systems use gyroscopes and accelerometers to measure the angular velocity, and linear acceleration of the navigating vehicle. A computer will then use integration from a known starting point to calculating position, heading and speed [2]. Optical gyroscopes, because they provide precise measurements of the angular velocity have been used to make very precise measurements of the rotation rate of the Earth [3].

2.2 Background

2.2.1 The Sagnac effect

When light is propagating through a ring rotating at angular velocity Ω the light will need to either travel slightly further to catch up with its original starting position, or it will meet with its starting position earlier than would be expected in a non-rotating cavity (depending on whether the direction of the light and the direction of the rotation are the same or opposite). In a ring cavity therefore the apparent cavity perimeter will be altered in the different directions [4] [5]. Resulting from this apparent length change is an apparent time advancement or delay to light in propagating in each direction. This advancement or delay can be expressed as:

$$t_{\pm} = \frac{2\pi R \pm \Delta P}{c} \quad (1)$$

where Δt_{\pm} is the time delay or advancement, R is the cavity radius, c is the speed of light and ΔP is the change in cavity perimeter is given by

$$\Delta P_{\pm} = R\Omega t_{\pm} \quad (2)$$

the cavity length changes due to rotation are therefore

$$\Delta P_{\pm} = \frac{2\pi R^2 \Omega}{c \mp R\Omega} \quad (3)$$

Where ΔP is the change in cavity perimeter, R is the radius of the cavity, c is the speed of light, and Ω is the gyroscope angular velocity. The resonance condition for optical cavities ($m\lambda=L$ where m is an integer) requires that the change in the optical path length will split the resonant frequencies based on the direction of propagation. by finding new using the resonance conditions of the cavity the frequencies can be calculated in the limit where $R\Omega \ll c$

$$f'_{\pm} = f_0 \pm \frac{A\Omega}{\lambda P} \quad (4)$$

Where f'_{\pm} are the new resonant frequencies, A is the area of the gyroscope cavity Ω is the angular velocity of the gyroscope, P is the perimeter of the ring cavity ($P=2\pi R$), and λ is the wavelength of light in the cavity. Therefore the splitting between the two new resonances can be expressed by the formula [5] [1]

$$\Delta f_{empty} = \frac{2A\Omega}{\lambda P} \quad (5)$$

where Δf_{empty} is the frequency splitting between the resonances of counter propagating beams in a rotating cavity in what are assumed to be "empty cavity" conditions, that is to say deviations of the index of refraction from vacuum are negligible as is optical dispersion (assumptions that will be reconsidered in 2.2.3). Optical gyroscopes operate by measuring the splitting between the resonant frequencies of counter propagating beams in a ring cavity to calculate angular velocity.

2.2.2 Laser Gyroscopes

This work considers a special class of optical gyroscopes: laser gyroscopes. The fundamental concept behind laser gyroscopes is fairly simple, a laser gyroscope is just an optical gyroscope that is also a laser. In its most simple form a laser is a gain medium in a cavity [1]. The gain medium amplifies incoming light, the amplified light is then cycled back into the amplifier which causes a positive feedback loop which will cause the total power of the light in the cavity to saturate due to the limited power output of the gain medium, some of the power is allowed to leak out through a partially transmissive mirror. The function of the laser cavity is not just to provide positive feedback, it also restricts the wavelength of the laser light to resonant frequency of the cavity. Laser light is therefore reasonably close to monochromatic and is at a frequency connected to the size of the cavity the gain medium is in.

A laser gyroscope consists of a gain medium inside of a ring cavity, thus, when rotated the laser will generate two counter propagating beams within the cavity which have frequencies locked to the resonances of the rotating cavity. In a laser gyroscope the frequencies of the fields inside of the cavity will be matched to the apparent path lengths of the cavity in counter propagating directions. Laser gyroscopes use these internally generated fields rather than some externally injected light source to find the resonant frequencies of the rotating cavity.

2.2.3 Fast Light

The theoretical consideration of the optical gyroscope presented earlier (2.2.1) was based on the assumption that the medium in the cavity had a refractive index of 1 ($n=1$) and was absent of any dispersions. The contributions of refractive index and dispersion are far from negligible. The resonance condition for optical cavities is not dependent on the absolute length of the cavity but instead on the optical path length of the cavity. Optical path length is concerned with phase shifts within light waves therefore the speed of light in that specific medium has a significant effect on path length. Mathematically, the optical path length is the product of the index of refraction and the absolute path length. the resonance condition for cavities then becomes

$$m\lambda = nP \quad (6)$$

where m is an integer, λ is the wavelength, P is the round trip length of the cavity and n is the index of refraction. Dispersions further complicate the matter, because in a dispersive material the speed of light, and therefore the index of refraction, have a dependency on frequency. Dispersion terms represent the first derivative of this dependency. The effects of dispersion on group index are shown below.

$$n_g = n_0 + f \frac{\partial n}{\partial f} \quad (7)$$

where n_0 is the refractive index, f is the frequency of light, and $\frac{\partial n}{\partial f}$ is the dispersion. The group index (n_g) is related to the group velocity in the same way that refractive index is related to wave velocity [6]

$$v_g = \frac{c}{n_g} \quad (8)$$

Which describes the velocity at which the envelopes of an optical signal propagates. The group velocity can be superluminal ($v_g > c$) under certain conditions as it does not necessarily carry information. This can be achieved by having a sufficiently negative dispersion such that $n_g < 1$, light propagating under this condition is referred to as fast light.

Theory predicts that the changes in the resonant frequencies due to a change in length are dependent on group velocity. In an empty cavity the resonance condition is

$$f = \frac{mc}{P} \quad (9)$$

where f is the frequency ($f = \frac{c}{\lambda}$), m is an integer and P is the length of the cavity. This condition implies that

$$\frac{F_0 + \Delta f}{f_0} = \frac{P_0}{P_0 + \Delta P} \quad (10)$$

employing the approximation $\frac{P_0}{P_0 + \delta P} = 1 - \frac{\Delta P}{P_0}$ yields

$$\frac{\Delta f}{f_0} = -\frac{\Delta P}{P_0} \quad (11)$$

the degree to which a length change in a cavity will change the resonant frequency is therefore

$$\Delta f = -\frac{f_0}{P_0} \Delta P \quad (12)$$

If a dispersive medium is added inside of the cavity then the resonance condition is

$$f = \frac{mc}{n(f)P} \quad (13)$$

where $n(f)$ is the refractive index in the dispersive medium at frequency f . This condition implies that

$$(f_0 + \Delta f)(n_0 + \Delta f \frac{\partial n}{\partial f})(P_0 + \Delta P) = f_0 n_0 P_0 \quad (14)$$

multiplying out and dropping terms that are second order in Δf this equation becomes

$$f_0 n_0 + f_0 \Delta f \frac{\partial n}{\partial f} + \Delta f n_0 = f_0 n_0 \frac{P_0}{P_0 + \Delta P} \quad (15)$$

applying the approximation $\frac{P_0}{P_0 + \Delta P} = 1 - \frac{\Delta P}{P_0}$ the equation simplifies to

$$f_0 \Delta f \frac{\partial n}{\partial f} + \Delta f n_0 = \frac{-\Delta L}{L_0} \quad (16)$$

a common factor of the group velocity can be pulled out on the left hand side.

$$n_g \frac{\Delta f}{f_0} = \frac{-\Delta P}{P_0} \quad (17)$$

the frequency shift per change in length of dispersive cavity is therefore

$$\Delta f = \frac{-f_0}{P_0 n_g} \Delta P \quad (18)$$

Comparing to equation 12, The frequency splitting in a dispersive cavity can be related to the frequency splitting in the empty cavity (where $n_0 = 1$) [7] [3]

$$\Delta f_{dispersive} = \frac{\Delta f_{empty}}{n_g} \quad (19)$$

In order to achieve the negative dispersion required to support fast light regimes the medium will have to display certain optical properties. The Kramers-Kronig relations describe the relationship between the index of refraction in a medium and the absorption of that medium. In order for strong negative dispersions to exist in a medium it must have an absorption like feature in the region of strong negative dispersion. In laser gyroscopes this tends to be problematic because laser gyroscopes require strong gain (at least exceeding unity) and strong absorption in the fast light region would mean that lasing will likely not be supported by the system. The ideal atomic system for generating fast light in medium will be strong amplification with a small dip that does not go below unity gain. Previous efforts have demonstrated that optical gain and steep dispersion can coexist in a particular N-bar four wave mixing scheme in the ^{87}Rb atomic structure where two pump fields tuned to the Rubidium D1 resonance 795nm (Ω_1) and the Rubidium D2 resonance 780nm (Ω_2) (see figures 1 and 2 for the full level structures) interact with the rubidium atoms and generate two new fields, each detuned by 6.8GHz from each of the pump fields.(see Figure 3) [8].

The strong gain and steep dispersion make this particular scheme a good candidate for use in laser gyroscope applications [9] [6].

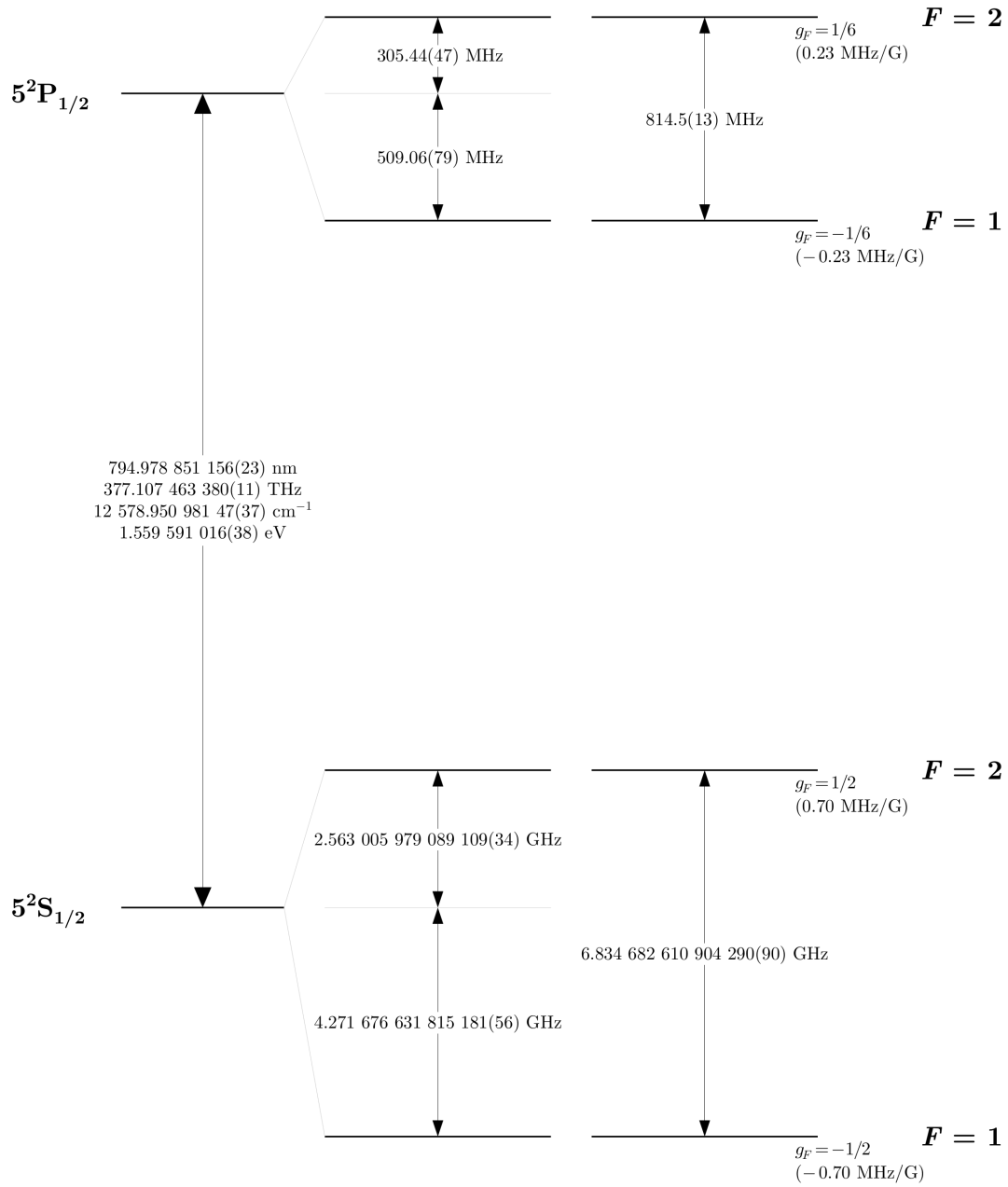


Figure 1: The level Scheme of the Rubidium D1 Resonance [10]

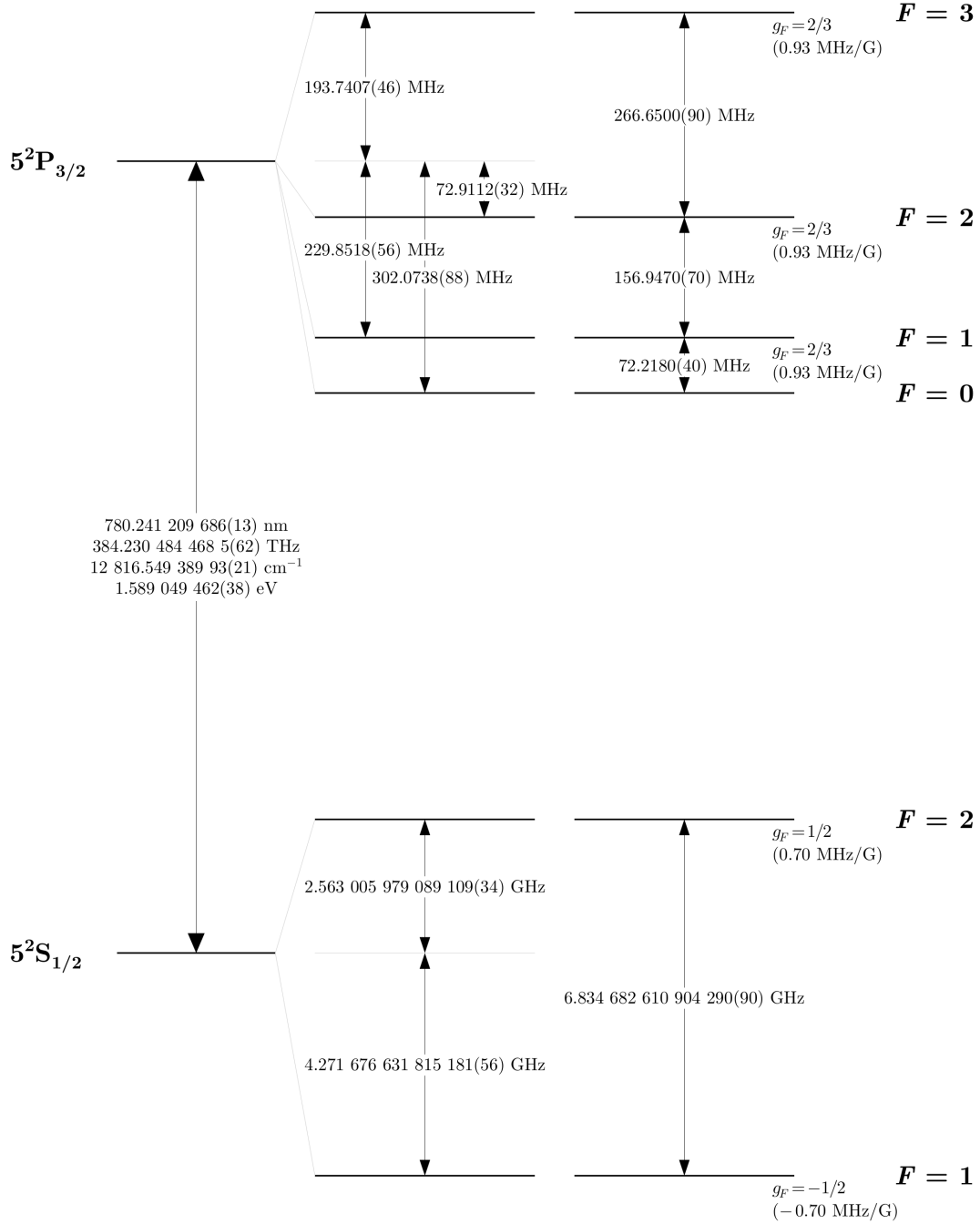


Figure 2: The Level scheme of the Rubidium D2 Resonance [10]

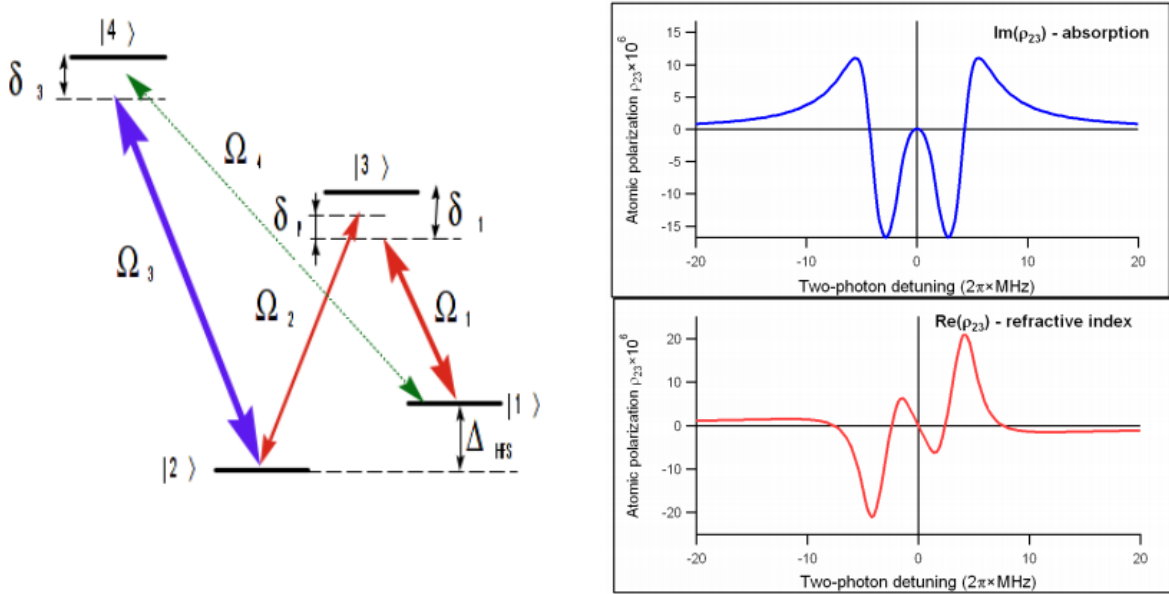


Figure 3: (Right) A simplified N-bar four wave mixing scheme to be tested as a medium provide gain for lasing as well as the conditions for fast light. (left) Predicted absorption and refractive index relations for this simplified four wave mixing scheme [8]

3 Experiment

3.1 Optical Apparatus

The gyroscope cavity used in this project consists of a square ring cavity containing a isotopically pure ^{87}Rb cell used to achieve four wave mixing to provide gain and strong negative dispersion. Four-wave mixing is induced in the Rubidium cell by injecting two pump fields (Ω_1 and Ω_3) tuned to the D1 and D2 Resonances of Rubidium (794.7 nm and 780 nm respectively). Two of the sides of the ring cavity are polarizing beam splitters, these ensure that the pump passes through the cell and is not circulated through the cavity, the polarizing beam splitters also allow some of the generated laser field to escape the cavity allowing for measurement of the internal field. (See Figures 4 and 5).

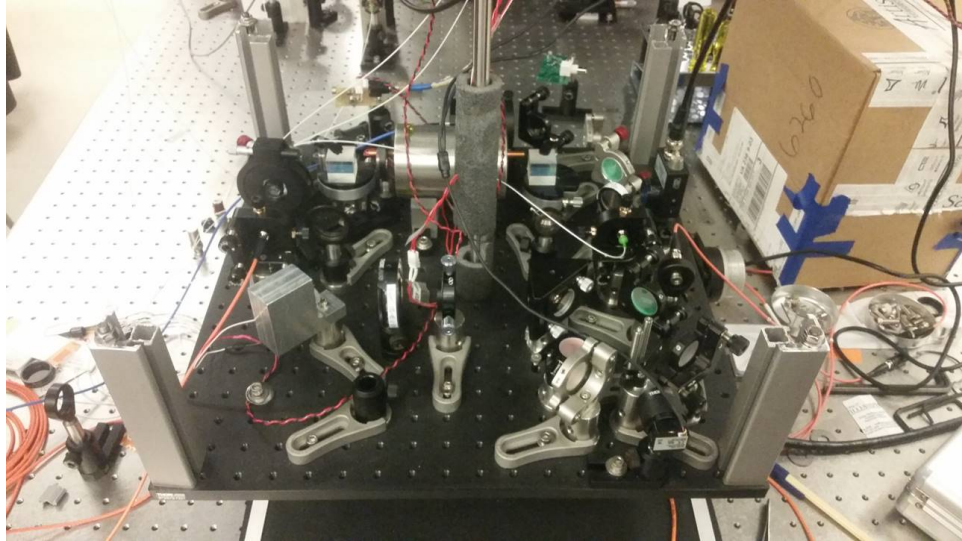


Figure 4: A Photograph of the ring cavity used for this research.

The degree to which the generated field is allowed to escape through the polarizing beam splitter is controlled by a quarter wave plate inside of the ring cavity. This quarter wave-plate controls the transmission of the cavity, and therefore controls the finesse of the cavity.

In order to provide measurements of rotational sensitivity the length of the cavity must be modulated, either through rotation or through the elongation of the cavity. One of the mirrors on the table was mounted to a piezoelectric, this mirror is used to electrically control cavity length.

Traditionally, in a simple linearly configured cavity, concave mirrors are used to ensure optical cavity stability. The ring cavity configuration used in this experiment is not conducive to the use of concave mirrors, so a lens placed inside of the cavity to maintain the stability of the system.

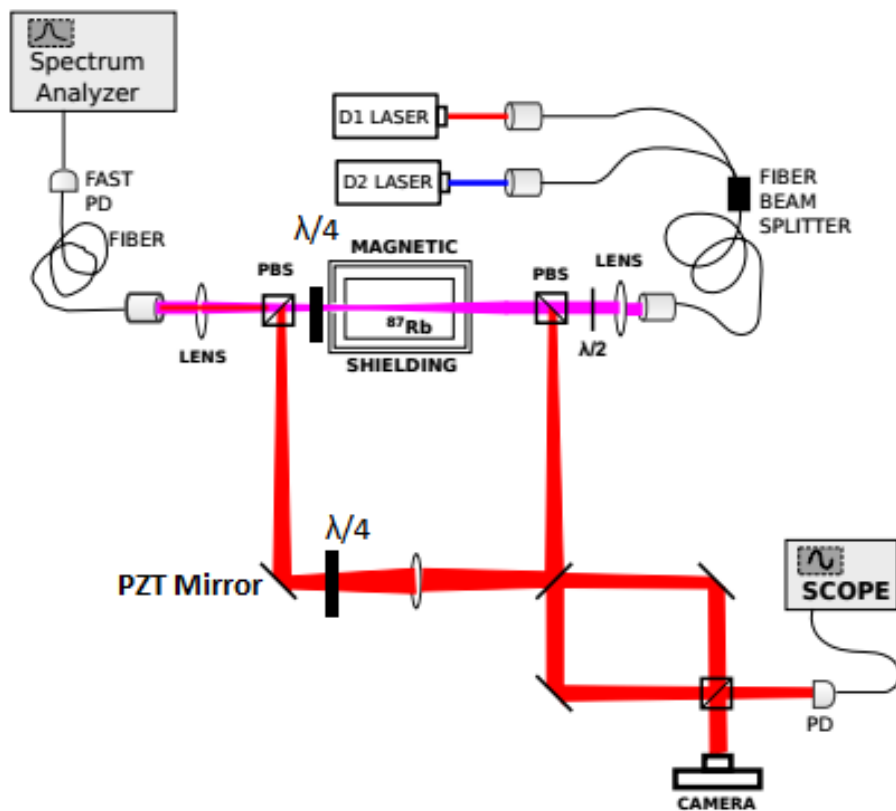


Figure 5: A simplified diagram of the cavity used in this experiment.

3.2 Measuring Gyroscope Sensitivity

An increase in gyroscope sensitivity would mean that smaller rotational velocities would register as a larger frequency splitting in the dispersive cavity than in the empty cavity, the magnitude of this increase in sensitivity can be characterized by a quantity henceforth referred to as pulling factor. The pulling factor is simply the ratio of the frequency change measured in the dispersive cavity to the frequency change expected in an empty cavity.

$$PullingFactor = \frac{\Delta f_{dispersive}}{\Delta f_{empty}} \quad (20)$$

based on the earlier theoretical considerations of the laser gyroscope, pulling factor should be equal to the inverse of the group index. In order to measure the sensitivity of the gyroscope, we measure the degree to which altering the length of the cavity effects the resonant frequencies of the cavity. Measuring the actual absolute frequency of the laser is extremely difficult. Instead of measuring the absolute frequency, heterodyne detection is used. Superimposing one of the pump fields with the generated gyroscope field a modulation of the optical power is induced near the hyperfine-splitting frequency of 6.83 GHz(see figure 6). This microwave frequency can be measured with relative ease using a fast photo-diode and a spectrum analyzer. Pulling factor is measured by the movement of beat note position while varying

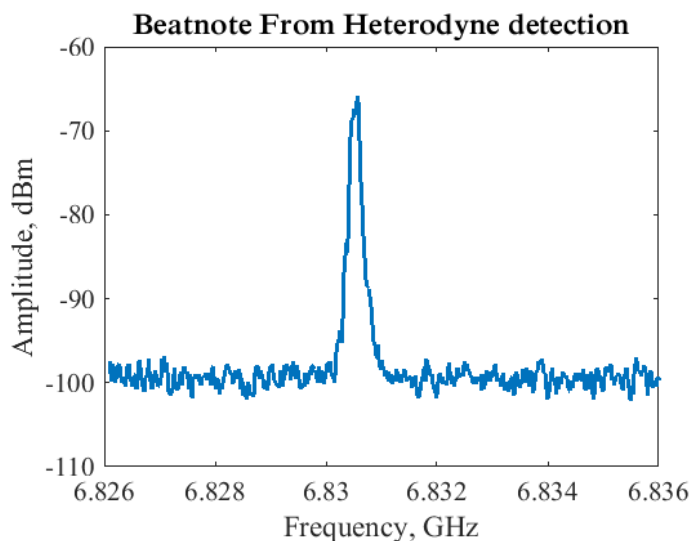


Figure 6: Typical Beat-note generated by mixing pump and lasing fields centered near 6.83 GHz.

the length of the cavity. Changes in cavity length can be readily converted into expected shifts in the resonant frequency of the empty cavity. The slope of the resulting data is the ratio of the measured dispersive cavity to the expected shift in an empty cavity, in other words the slope is the pulling factor.

(see figure 7) Pulling factor is therefore extracted from data by fitting a line to the data and taking the slope.

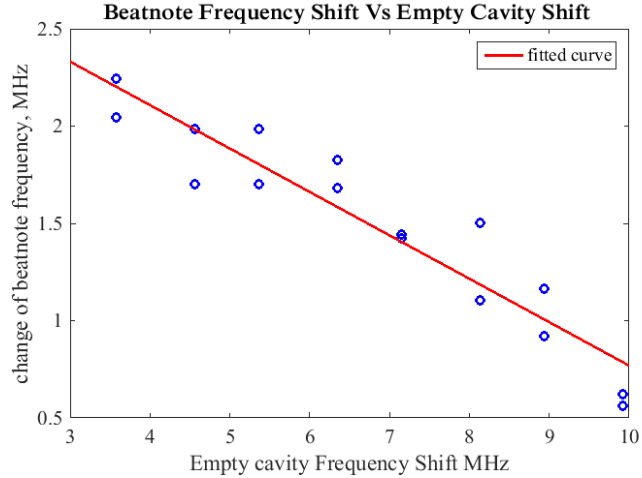


Figure 7: Beat-note measurements at different cavity lengths

3.3 Control Systems

In order to properly control the parameters necessary for the experiment a number of control systems had to be applied.

Control of cavity length proved to be particularly particularly important. A proportional-integral controller is used to stabilize the cavity length. Initially, generation features from four wave mixing were used as lock signals, these signals tended to be very abrupt and tended to cease to be linear beyond a certain range, this meant that they were not effective candidates for locking signals. In order to stabilize the cavity length effectively, a third field(referred to as the lock field), far detuned from rubidium resonances, was injected into the cavity, the resonances of this field were used as a lock signal. By slowly modifying the detuning of the lock field, the length of the cavity can be stably controlled.

To fully explore the parameter space of the four wave mixing, careful control of the pump detuning is required as well. In order to measure pump detuning a reference cavity was used. The length of the reference cavity can be stably modulated using a high voltage signal. Calibration measurements of the reference cavity were made allowing for conversion between voltage changes, and length changes. By positioning a reference cavity resonance on top of a known atomic resonance and then altering the reference cavity length to move the resonances to the desired detuning. The use of this reference cavity allows for the calibrated detuning of pump fields. This system can was sometimes used in conjunction with a PID controller to stabilize pump detuning.

3.4 Pump Power Control

Controlling the pump power in the experiment was first conducted by attenuating the pumps before injecting them through the rubidium cell. This method proved to place fairly stringent limitations on the experiment. The relatively weak external cavity diode lasers used as sources for the pump fields were further attenuated as they incurred losses when injected into optical fibers. The highest combined pump power achievable using this method were limited to a maximum around 10 mW. In order to increase the power of the system a semi-conductor amplifier system was added. The combined pumps are injected through a fiber into the laser amplifier and then through the gyroscope cell. The semiconductor amplifier increased the maximum pump power to a level of 200 mW.

4 Results

The parameters theorized to have an effect on the properties of this four wave mixing scheme are numerous. Factors like pump power, pump power ratio, rubidium vapor density, pump detuning, and cavity finesse are hypothesized to have strong effects on pulling factor. The dependences are not necessarily independent of one another, altering one parameter may have drastic effects on the dependencies on other parameters. As a result dependences are measured in different regimes. As a target a pulling factor of greater than one would mean that the sensitivity of the gyroscope has exceeded the empty cavity regime.

Pulling factor measurements are directly correlated with the sensitivity of the gyroscope. In addition to pulling factor measurements measurements of beatnote amplitude were taken. Beatnote amplitude is related to the amount of power in the laser fields. Beatnote amplitude provides a measurement of the power of the lasing. Generally higher laser power translates to simpler detection algorithms.

4.1 Low Power Regime

The first experiments were carried out before the addition of the semiconductor amplifier. Power in these first experiments was limited to approximately 10mW of total pump power.

4.1.1 Initial D1 Detuning Dependence

The first parameter dependence to be evaluated systematically was the D1 pump detuning. While measuring the initial D1 detuning dependence, the D2 pump was tuned to the peak generation at $F_g = 2 \rightarrow F_e = 1$ transition. The D2 pump had 2 mW of power inside the cell while the D1 pump

had a power of 5 mW inside of the cell. The rubidium cell was at a temperature of 80 degrees Celsius. Measurements of pulling factor, and peak beat note amplitude were taken at various D1 detunings, (see figures 8 and 9)

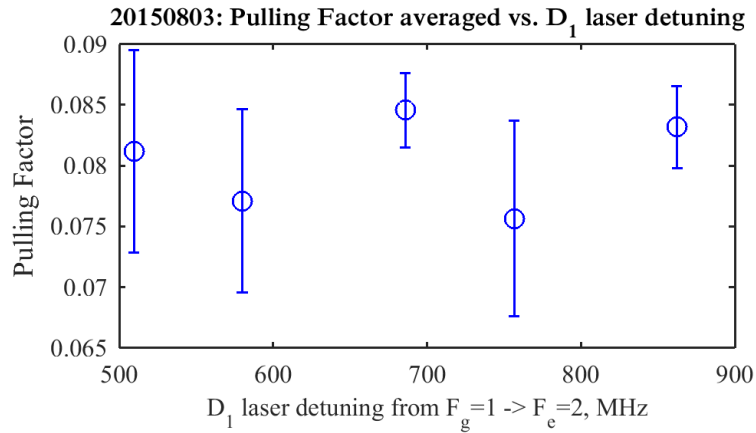


Figure 8: The initial Dependence of pulling factor on D1 pump detuning

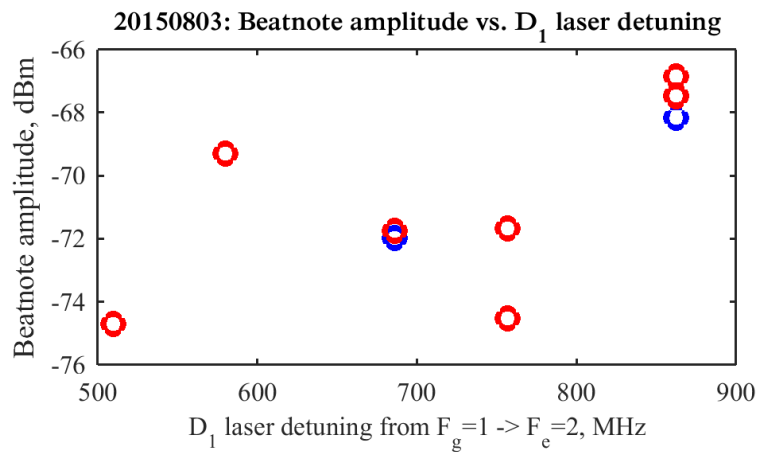


Figure 9: The initial dependence of beat-note amplitude on D1 pump detuning.

In this regime the dependence of pulling factor on D1 Detuning appeared to be rather weak despite the detuning range of nearly 400 MHz pulling factors all are clustered fairly neatly between 0.075 and 0.085 with fairly broad error bars. Beatnote amplitude, like pulling factor did not show a strong dependence on D1 detuning under these conditions.

4.1.2 Initial D2 Detuning Dependence

After measuring very little dependence of pulling factor on D1 Detuning under the previous conditions, the D2 pump detuning was the next parameter to be evaluated. For the duration of this particular experiment the D1 pump was tuned 684 MHz away from the $F_g = 1 \rightarrow F_e = 2$ transition. The D1 pump was injecting a 5mW of power into the rubidium cell, while the D2 pump was injecting around 2mW into the cell. The rubidium cell temperature was maintained at 80 Degrees Celsius. As in the previous experiment, measurements of beatnote amplitude were taken at various D2 detunings (See Figures 10 and 11)

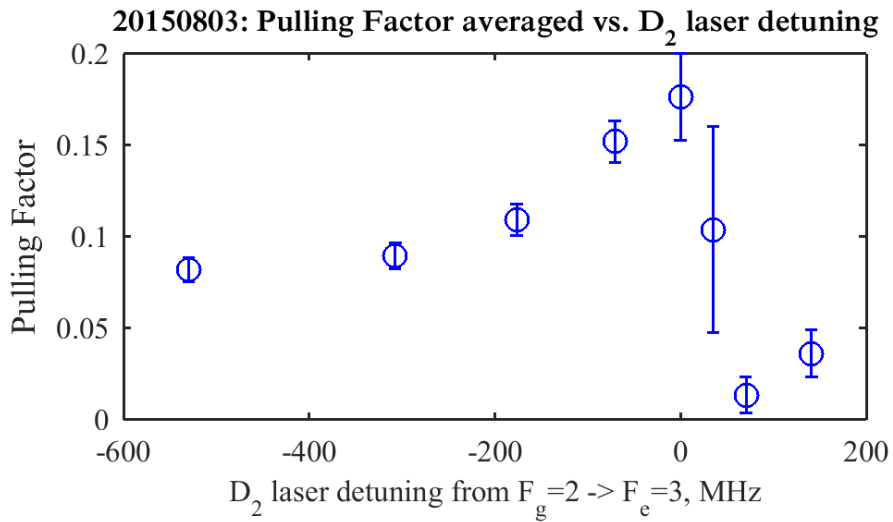


Figure 10: The initial dependence of pulling factor on D2 pump detuning

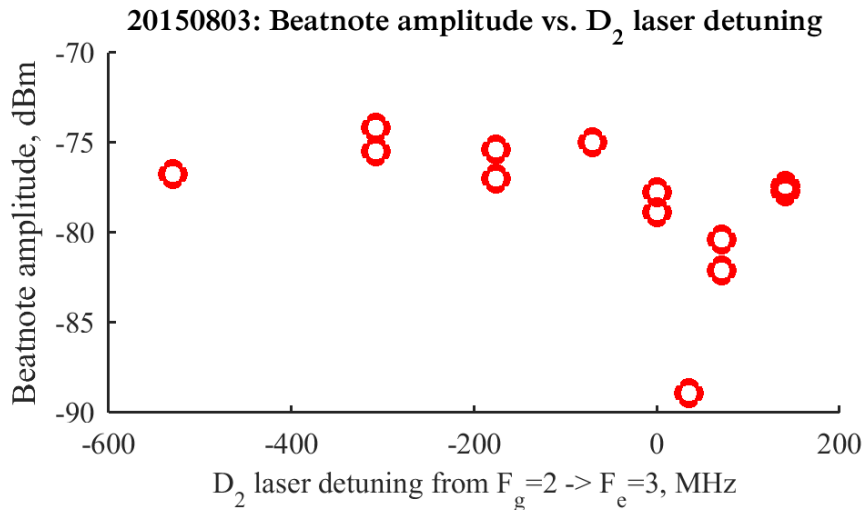


Figure 11: Beatnote amplitude dependence on D2 detuning

In a contrast to the initial D1 pump detuning dependence the D2 pump detuning dependence was fairly strong. When the D2 pump was tuned to the $F_g = 2 \rightarrow F_e = 3$ transition pulling factor was double what it was when it was detuned 600MHz to the negative, and at least an order of magnitude larger than when detuned 75Mhz to the positive. Beat note amplitude began to roll off right around the area of strong pulling factor but dropped to its weakest point just before entering the region of low pulling factor (see figure 10).

4.1.3 D1 Detuning Dependence under improved D2 Detuning Conditions.

After Maximizing the pulling factor with the D2 pump detuning under previous conditions. D1 dependence was re-evaluated under the new slightly improved conditions. For this experiment the D2 pump was tuned to the $F_g = 2 \rightarrow F_e = 3$ transition, where maximum pulling factor was observed in the previous experiment. The D2 pump was injecting 2 mW of power into the cell, and the D1 pump was injecting 5mW of power into the cell. the rubidium cell temperature was 80 degrees Celsius. Measurements of pulling factor, and peak beat note amplitude were taken at various D1 detunings (see figures 12 and 13)

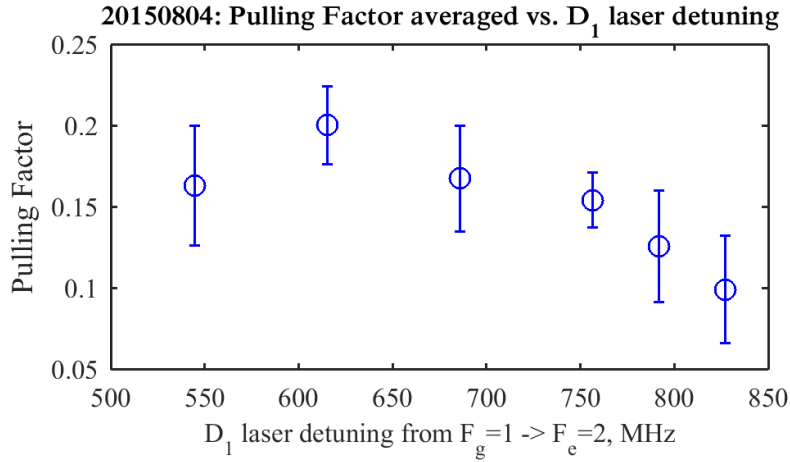


Figure 12: dependence of pulling factor on D1 Detuning under improved D2 detuning conditions

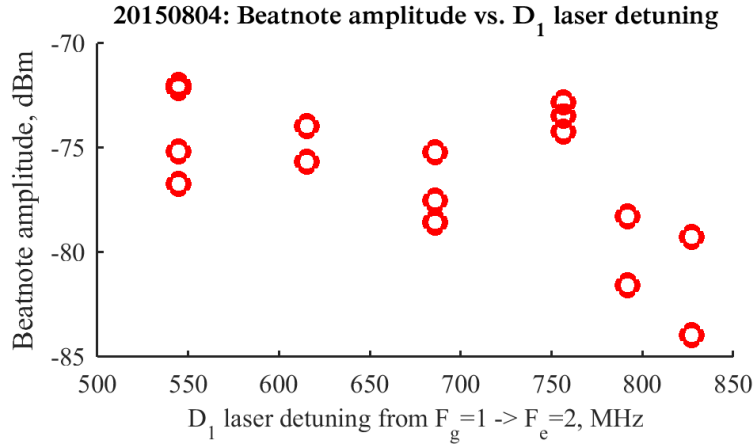


Figure 13: dependence of beat-note amplitude on D1 pump detuning under improved D2 detuning conditions

With the new D2 pump Detunning the effect of D1 detuning became more apparent. Pulling factor was maximized when D1 was detuned 600 MHz from the $F_g = 1 \rightarrow F_e = 2$ transition. In contrast to the

D2 dependence, the D1 dependence did not display a sharp drop in pulling factor. Beatnote amplitude does not appear to be strongly correlated with pulling factor in this regime.

4.1.4 D2 Power Dependence

Pump power is hypothesized to have a strong effect on pulling factor [6]. In this configuration the easiest power parameter to adjust was D2 pump power. Power was altered by attenuating the D2 pump before it is injected into the rubidium cell. The D1 pump was tuned 684 MHz away from the $F_g = 1 \rightarrow F_e = 2$ transition while providing 5mW of power into the cell. the D2 pump was tuned to the $F_g = 2 \rightarrow F_e = 3$ transition, where maximum pulling factor was measured. Pulling factor and beat note amplitude were measured at various D2 pump powers (see figures 14 and 15).

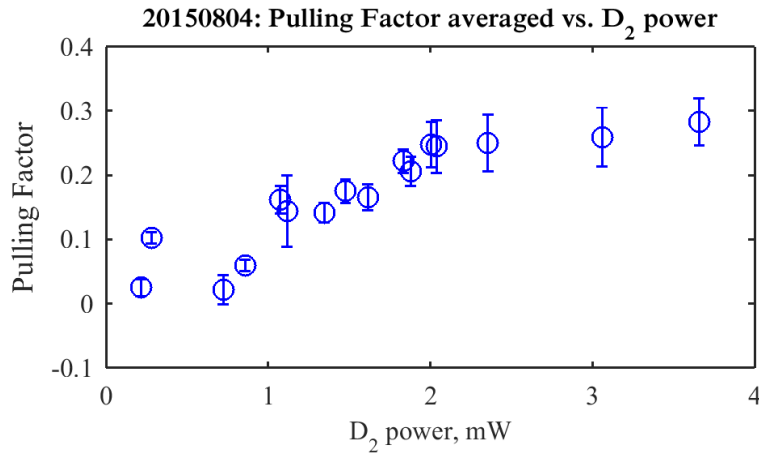


Figure 14: The dependence of pulling factor on D2 pump power

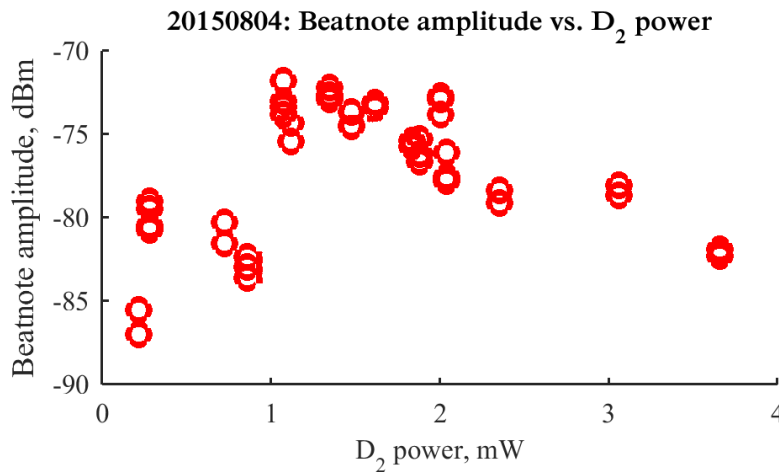


Figure 15: Dependence of beatnote amplitude on D2 Power

As the D2 pump power was increased, the pulling factor continued to increase. There was no observed maximum in this dependence. It is unclear from the observed dependence whether increasing pump power would continue to cause drastic improvements to pulling factor or if increasing the power would just bring pulling factor closer to an asymptotic limit. At higher powers where higher pulling factor was observed the beat note amplitude was beginning to roll off.

4.1.5 Vapor Density Dependence

Temperature directly effects the density of the vapor in the ^{87}Rb vapor in the cell. The density of the ^{87}Rb vapor is theorized to have an effect on pulling factor. The temperature was controlled via a temperature controller that regulates the temperature of the rubidium cell. From the temperatures of each experiment the optical density can be easily calculated [10]. The pump fields were tuned to maximize generation. Pump powers were maintained at the levels of previous experiments, the D2 pump was injecting 2mW into the cell while the D1 pump was injecting 5 mW. Pulling factor and beat note amplitude were measured at various temperatures (see figures 16 and 17).

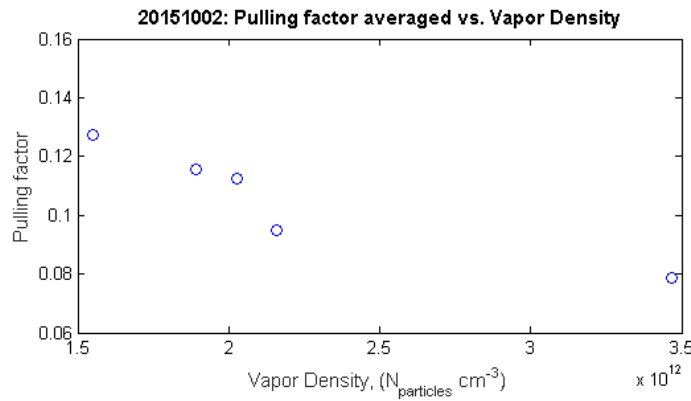


Figure 16: Dependence of pulling factor on Vapor Density

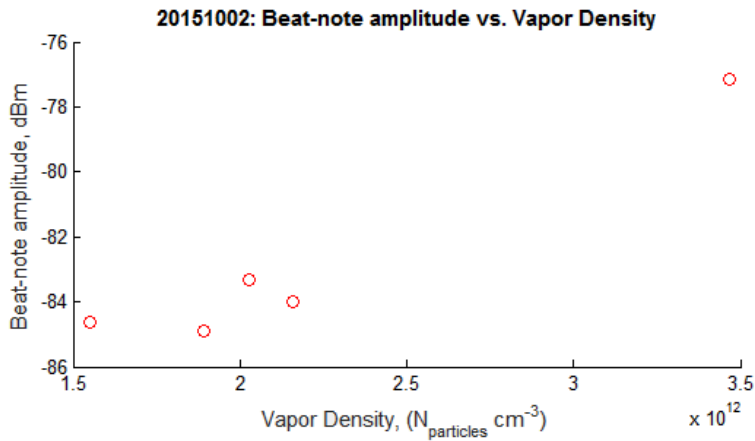


Figure 17: Dependence of Beatnote Amplitude on Vapor Density

At these detunings and powers increasing the vapor density caused fairly drastic drops in pulling factor. Increasing the temperature by 20 degrees the nearly dropped the pulling factor by nearly half. While decreasing pulling factor, increased vapor densities caused fairly strong increases to beat note

amplitude.

4.1.6 Finesse Dependence

Finesse is also theorized to have an effect on pulling factor. In this experiment some losses are required to measure the generated field, therefore higher finesse make measurements more difficult. However, a high finesse is hypothesized to have strong contributions to pulling factor. To test the dependence, the pump fields were tuned to maximum generation and measurements of pulling factor and beatnote amplitude were taken after varying the finesse (figure 18 and 19). Finesse was controlled by rotating a quarter wave plate that controls losses in the generated field inside the cavity (see figure 5).

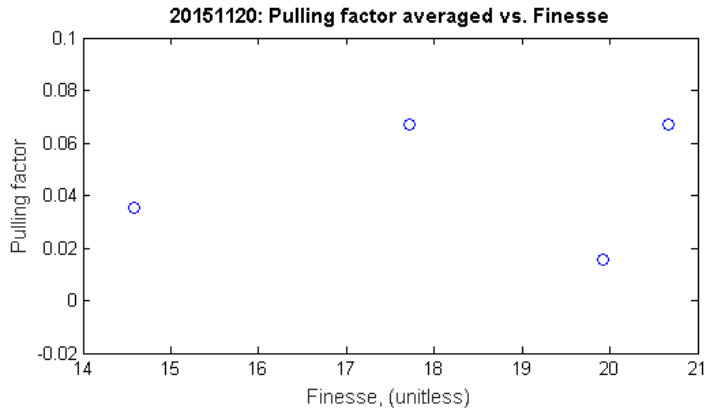


Figure 18: Dependence of pulling factor on finesse.

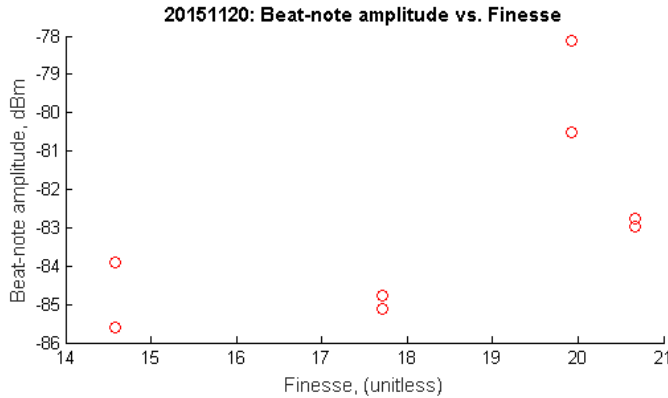


Figure 19: Dependence of beatnote amplitude on finesse.

The wave plate rotations conducted, represent a fairly wide range in finesse (nearly a 50 percent variation). Contrary to expectations pulling factor was lowest at the point of highest finesse (polarizer position: 203 Degrees).

4.1.7 Low Power Conclusions

The most drastic conclusion from the low power regime was the observation that pump power has a strong effect on pulling factor. After the completion of these experiments it became apparent that higher powers were required to achieve higher pulling factors.

4.2 High Power Regime

Power was increased using a semiconductor laser amplifier. Using this device much higher powers became achievable. Powers reaching as high as 200 mW became possible with the application of the amplifier. The Amplifier did, however, add a layer of increased complexity to the experiment. After adding the amplifier more and more time was spent ensuring the functionality of the setup.

4.2.1 D2 detuning Dependence (High Power Regime)

The addition of a semiconductor laser amplifier to system allows for pump powers an order of magnitude higher than in the previous experiments. The first dependence measured with the inclusion of the semiconductor amplifier was the dependence on D2 pump detuning. The D1 pump was detuned +1.5 MHz away from the $F_g = 1 \rightarrow F_e = 2$ resonance. The total pump power injected into the cell was 181 mw with a distribution of 58% of the power coming from D1 and 42 % coming from D2. Measurements of pulling factor and beatnote amplitude were made at various D2 pump detunings (Figures 20 and 21).

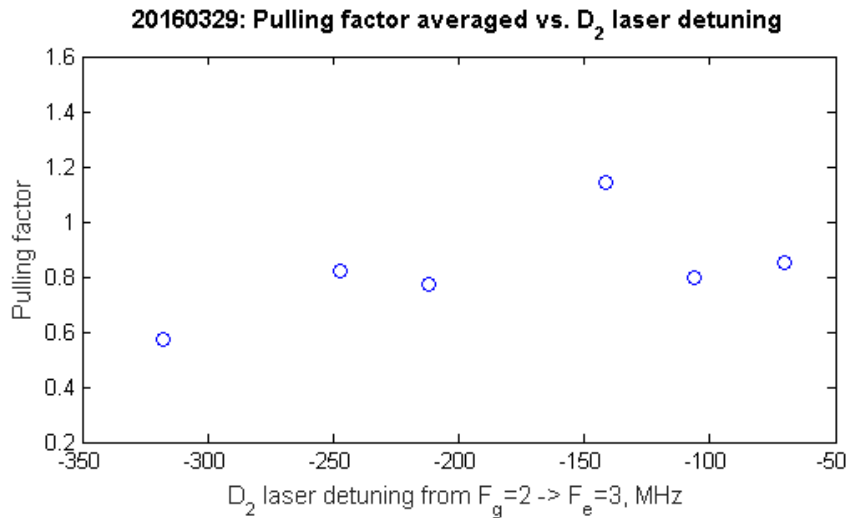


Figure 20: Pulling factor dependence on D2 Detuning in the high power regime

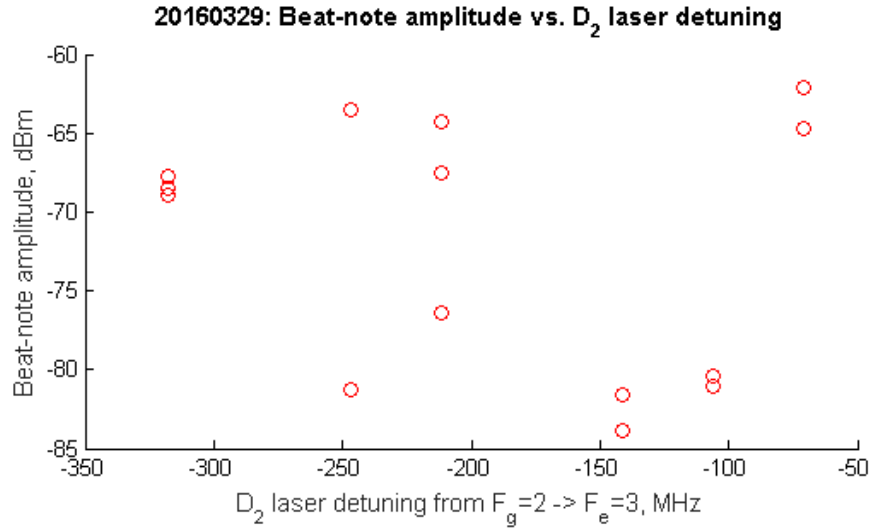


Figure 21: Dependence beat-note amplitude on D2 detuning in the high power regime.

In the low power regime (total pump power 10 mW), pulling factors were limited to around 0.3. Increasing the power allowed for drastic improvements to pulling factor, the minimum pulling factor observed in this experiment was around 0.6 nearly double the maximum pulling factor observed in the low power experiments. The pulling factor approached and may have exceeded the limiting pulling factor of one. In addition to the strong improvement to pulling factor, the increased pump power provided for significantly stronger beatnote signals.

4.2.2 Pump Power Dependence

Previous experiments revealed that pump power has an enormous effect on pulling factor. The use of the semiconductor amplifier allows for a greater range of powers than provided in the low power regime, this allows the dependence to be tracked over a larger range. When measuring the dependence of pulling factor on total pump power, pump power was controlled by changing the gain on the semiconductor amplifier. The temperature of the cell was set at $90\text{ }^{\circ}\text{C}$ during the duration of the test. The pump power distribution was skewed toward D1 so that $2/3$ of the power came from D1 and the other third came from D2. The D1 pump was tuned $+1.5\text{GHz}$ away from the $F_g = 1 \rightarrow F_e = 1$ and The D2 pump was tuned -150 MHz from $F_g = 2 \rightarrow F_e = 3$ where maximum pulling factor was observed in the high power regime D2 detuning experiment. Under these conditions, the pulling factor and beatnote amplitude were measured at various powers (figures 22 and 23).

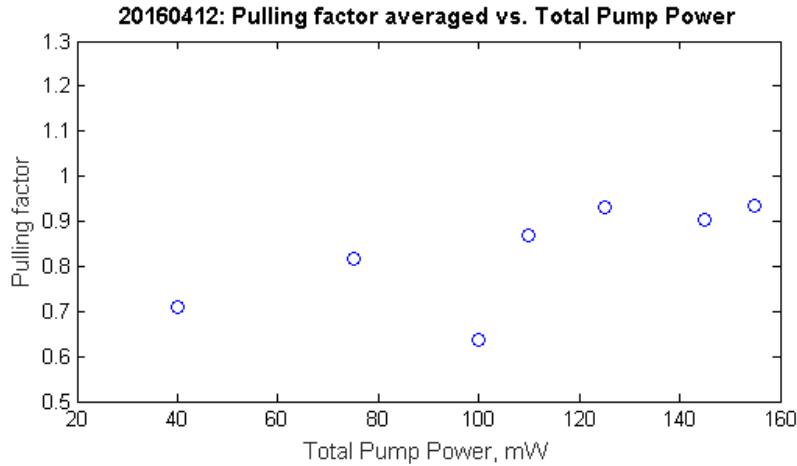


Figure 22: Pulling factor dependence on total pump power in the high power regime

As pump power increased so to did the pulling factor. Maximum pulling factors (near unity) were measured at higher powers. As pulling factor increased at higher powers, beat note amplitude began to roll off as with other tests.

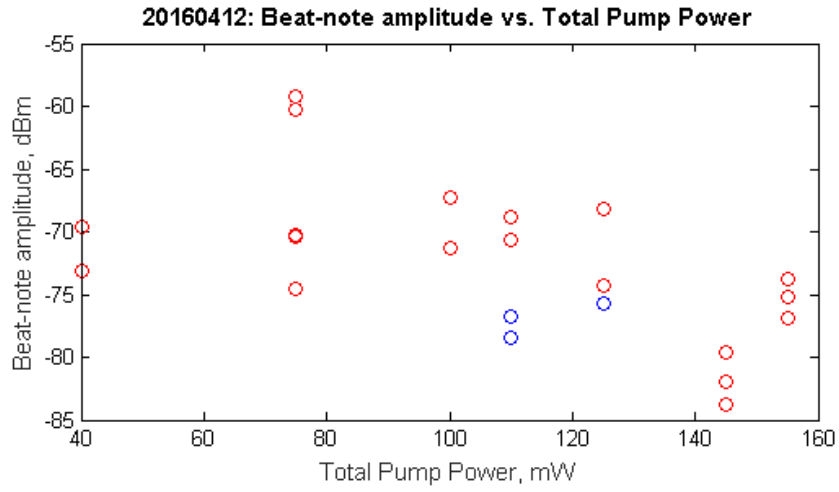


Figure 23: Final dependence beat-note amplitude on total pump power

4.2.3 High Power Conclusions

In the high power regime, it is not as self evident what the path forward is. It is yet unclear whether or not pulling factor will asymptotically approach one at higher and higher powers or if it will be able to exceed the observed maximum of unity.

5 Discussion

The properties of the optical gyroscope cavity under consideration in this experiment are sensitive to a wide range of factors.

The most obvious dependence was the strong dependence of pulling factor on power. Across the board it appears that increasing pump power increases the pulling factor. Seemingly, just by increasing the pump power pulling factors can be brought from near 0 to approaching unity. In addition to the improvement of pulling factor the higher pump powers correspond to higher powers of the field generated within the cavity, the high power of the gyro field corresponds to a higher beatnote amplitude and therefore detection of the beatnote is easier. Increased power seems to be the easiest parameter to modify to achieve large pulling factors.

Although higher pump powers yield to both higher pulling factor and a higher beatnote amplitude it appears that the connection between the two properties of the gyro signal are not necessarily correlated. Increasing the density of the rubidium vapor caused the pulling factor to drop while increasing the beatnote amplitude.

Detuning dependences seem to be more strongly dependant on the other parameters in the system. The pump detuning dependences were altered by factors such as the power of the pumps and the detuning of the other pump.

The sensitivity of the gyroscope can be calculated based on equation 5. The sensitivity of the gyroscope is

$$\Delta\Omega = \frac{\Delta f \lambda P}{2A} \frac{1}{PF} \quad (21)$$

The cavity has a Perimeter of 0.8m and An area of $0.04m^2$. In this case Δf is the uncertainty of beatnote frequency measurements. Estimating by looking at the distribution of points in figure(4), 0.5 MHz is a reasonable estimate of frequency uncertainty. With a wavelength of approximately 800 nm the sensitivity is approximately

$$\Delta\Omega = \frac{0.4 \frac{Rad}{sec}}{PF} \quad (22)$$

The gyroscope sensitivities in this experiment ranged from a lower bound of $8 \frac{Rad}{sec}$ (PF 0.05) to near $0.4 \frac{Rad}{sec}$ (PF 1).

6 Conclusions

Tuning various parameters can have very drastic effects on the sensitivity of this gyroscope cavity. Most notably higher power regimes tend to provide improved sensitivity. Further improvements can make the cavity very sensitive. Despite low initial pulling factor observations of around 0.1, tuning parameters especially power and pump detuning can drive pulling factors to approach unity. Further exploration of the parameter space may lead to pulling factors reliably greater than unity.

7 Acknowledgments

This material is based upon work supported by the National Science Foundation under Grant No. 1359364 and Naval Air Warfare Center STTR program, contract N68335-13-C-0227. Matt Simons, and Jesse Evans did much of the ground work upon which this research is based. ShuangLi Du provided a significant amount of assistance with the experiment.

References

- [1] Adi Shamir. An overview of optical gyroscopes theory, practical aspects, applications and future trends. 2006.
- [2] The Editors of Encyclopdia Britannica. Inertial guidance system. *Encyclopdia Briannica*, 2015.
- [3] K. Salit M. Salit, G. S. Pati, , and M. S. Shahriar. Fast-light for astrophysics: super-sensitive gyroscopes and gravitational wave detectors. *Journal of Modern Optics*, 54(1):24252440, 2007.
- [4] E.J. Post. Sagnac effect. *Reviews of Modern Physics*, 39(3), 1967.
- [5] Jesse Evans. Implementation and evaluation of four wave mixing in optical gyroscopes. *The College Of William and Mary (Honors Thesis)*, 2014.
- [6] Irina Novikova; Eugeny E. Mikhailov; Logan Stagg; Simon Rochester; Dmitry Budker. Tunable lossless slow and fast light in a four-level n-system. *SPIE Proceedings*, 8636, 2013.
- [7] Shahriar et al. Ultrahigh enhancement in absolute and relative rotation sensing using fast and slow light. *Physical Review A*, 75(053807), 2007.
- [8] Dmitry Budker Simon M. Rochester Eugeny E. Mikhailov, Jesse Evans and Irina Novikova. Four-wave mixing in a ring cavity. *Optical Engineering*, 53(10), 2014.
- [9] Eugeny E. Mikhailov Dmitry Budker Nathaniel B. Phillips, Irina Novikova and Simon M. Rochester. Controllable steep dispersion with gain in a four-level n -scheme with four-wave mixing. *Journal of Modern Optics*, 60:64–72, 2013.
- [10] Daniel A. Steck. Rubidium 87 d line data. 2008.